One- and Two-Photon Fluorescent Polyhedral Oligosilsesquioxane (POSS) Nanosensor Arrays for the Remote Detection of Analytes in Clouds, in Solution, and on Surfaces

Claire Hartmann-Thompson,*,† Douglas L. Keeley,† Kathleen M. Pollock,† Petar R. Dvornic,† Steven E. Keinath,† Marcos Dantus,‡ Tissa C. Gunaratne,‡ and Dale J. LeCaptain§

Michigan Molecular Institute, 1910 West St. Andrews Road, Midland, Michigan 48640-2696, Department of Chemistry, Michigan State University, East Lansing, Michigan 48824-1322, and Department of Chemistry, Central Michigan University, Mount Pleasant, Michigan 48859

Received December 20, 2007. Revised Manuscript Received January 30, 2008

A series of polyhedral oligosilsesquioxane (POSS) nanosensors functionalized with fluorophores that change their wavelength of emission in response to their chemical environment has been synthesized and characterized by IR, NMR, UV, one- and two-dimensional fluorescence spectroscopy, MALDI-TOF MS, and electrospray MS. When each nanosensor in an array of *n* nanosensors is functionalized with a different wavelength shifting fluorophore, the array can generate a unique fingerprint comprised of *n* emission wavelength data points in response to a given chemical warfare agent (CWA) simulant or toxic industrial chemical (TIC). One-photon fluorescence fingerprints were constructed by measuring the fluorescence spectra of nanosensor−analyte pairs in solution. Two-photon fluorescence fingerprints were then generated by remotely interrogating nanosensor−analyte pairs using a femtosecond IR laser and a stand-off fluorimeter. Two-photon fingerprints were obtained for analytes in solution, on a surface, and in cloud form. A four-component nanosensor array could differentiate a homologous series of alcohols and distinguish G and VX classes of nerve agent simulants.

Introduction

At the most general level, stand-off sensing techniques must function either by passive detection of waves emitted from remote objects (e.g., passive FTIR), or by actively sending a wave to a remote object, and obtaining information by analyzing the wave(s) returning from the object (e.g., laser detection and ranging, LIDAR). An early report[1] on the topic of stand-off detection of air pollutants correctly foresaw that the major technical obstacles in remote detection would be scattering caused by solid particles or droplets and measurement of low-energy signals against a complex and constantly changing background. This challenge has traditionally been addressed by modifying the detection system and designing ever more powerful and sophisticated instrumentation and data processing algorithims.[2–4] However, an alternative strategy is to modify the remote location itself, such that the location is able to send higher-quality information back to the sensor. For example, enhanced Raman spectroscopy has been developed where colloidal silver or gold nanoparticles have been sprayed onto a surface to improve the quality of the signal it generates, and the surface has been remotely interrogated using a Raman telescope at a distance of 5 meters.[5] Another way to enhance the quality of information arriving from the remote location is to introduce fluorophoric nanoparticles at the remote location and use the nanoparticles to generate fluorescence signals that give information about the chemical composition of their immediate vicinity.

In this study, a set of polyhedral oligosilsesquioxane (POSS) nanosensors designed to change their wavelength of fluorescence emission upon interaction with analytes was synthesized and characterized (Figure 1). A four-component array of nanosensors was used to generate fluorescence data sets (fingerprints) for a number of analytes including chemical warfare agent (CWA) simulants and toxic industrial chemicals (TICs) by measuring the one-photon fluorescence spectra of nanosensor−analyte pairs. The feasibility of using the nanosensor array for the remote detection of analytes in clouds and on surfaces was then evaluated. A femtosecond laser was used to interrogate the array and induce two-photon fluorescence in the nanosensors, and a remote fluorescence probe was used to record the responses of the nanosensors.

* Corresponding author. E-mail: thompson@mmi.org.
† Michigan Molecular Institute.
‡ Michigan State University.
§ Central Michigan University.

(1) Ludwig, C. B.; Bartle, R.; Griggs, M. *Study of Air Pollutant Detection by Remote Sensors*; Contract Report NASA CR-1380; National Aeronautics and Space Administration: Washington, D.C., 1969.
(2) Tarumi, T.; Small, G. W.; Combs, R. J.; Kroutil, R. T. *Appl. Spectrosc.* **2003**, *57* (11), 1432–1441.
(3) Avishi, B. D. *Opt. Express* **2003**, *11* (5), 418–429.
(4) Cosofret, B. R.; Marinelli, W. J.; Ustun, T. E.; Gittins, C. M.; Boies, M. T.; Hinds, M. F.; Rossi, D. C.; Coxe, R. L.; Chang, S. D.; Green, B. D.; Nakamura, T. *Proc. SPIE* **2004**, *5584* (Chem. Bio. Standoff Detection II), 93–99.
(5) Hernandez-Riviera, S. P.; Pacheco-Londono, L. C.; Ortiz, W.; Rivera-Batancourt, O. *Abstracts of Papers, 23th ACS National Meeting*., Boston, MA, Aug 19–23; American Chemical Society: Washington, D.C., 2007.

10.1021/cm703641s CCC: $40.75 © 2008 American Chemical Society
Published on Web 03/21/2008

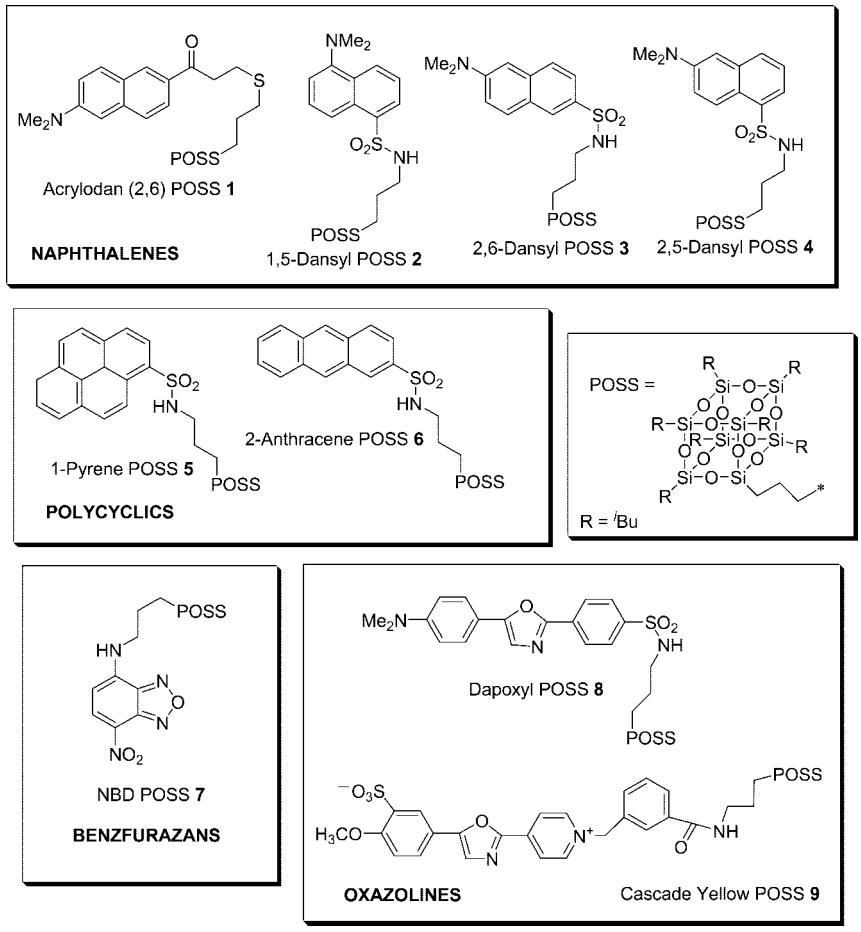

Figure 1. Polyhedral oligosilsesquioxanes (POSS) functionalized with fluorophoric sensor groups that change their fluorescence emission wavelength in response to their chemical environment.

POSS compounds are derivatives of trifunctional silanes of the form $RSiX_3$[6,7] and are prepared in hydrolysis–condensation reactions. These reactions can generate a variety of products depending on silane and water concentration, pH, temperature, solubility, and catalyst.[8] The nanoscopic polyhedral oligosilsesquioxanes used in this study are stoiciometrically well-defined closed cage structures of the form $R_8Si_8O_{12}$ (Figure 1) and may be considered a nanoscale form of silica. POSS compounds are ideal scaffolds for sensor groups because they are of a precisely defined size, they are commercially available with a variety of functional groups, and they have been used in a wide range of applications in the past few years.[9–12] POSS has been functionalized with fluorescent dyes in order to prepare light-emitting materials,[13,14] and light-emitting POSS-containing polymers and three-dimensional networks are also known.[15,16] POSS functionalized with hydrogen-bond acidic sensor groups has been used as a nanoadditive in coatings for surface acoustic wave (SAW) sensors,[17] but there is no precedent for the use of POSS systems functionalized with fluorescent dyes in a fluorescent sensor array application.

The fluorescent labels of Figure 1 (acrylodan,[18] dansyl,[19] anthracene and pyrene,[20] NBD,[21] dapoxyl[22] and Cascade Yellow[23]) were selected for this study because they are commercially available in forms that react with amino and

(6) Scott, D. *J. Am. Chem. Soc.,* **1946**, *68*, 356.
(7) Voronkov, M. G.; Lavrent'yev, V. I. *Top. Curr. Chem.* **1982**, *102*, 199–236.
(8) Brinker, C. J.; Scherer, G. W. *Sol−Gel Science: The Physics and Chemistry of Sol−Gel Processing*; Academic Press: San Diego, 1990.
(9) Feher, F. J.; Budzichowski, T. A. *Polyhedron* **1995**, *14*, 3239–3253.
(10) Lichtenhahn, J. D. In *Polymeric Materials Encyclopedia*; Salamone, J. C., Ed.; CRC Press: Boca Raton, FL, 1996; Vol. 10, pp 7768–7778..
(11) Pielichowski, K.; Njuguna, J.; Janowski, B.; Pielichowski, J. *Adv. Polym. Sci.* **2006**, *210*, 225–296.
(12) Phillips, S. H.; Haddad, T. S.; Tomczak, S. J. *Curr. Opinion in Solid state Mater. Sci.* **2004**, *8*, 21–29.
(13) Cammack, J. K.; Jabbour, G. E.; Li, S.; Froehlich, J. 2005,U.S. Patent 0123760 A1.
(14) Lee, M. W.; Kim, S.; Furman, B. R.; Brick, C.; Laine, R. M. *Abstracts of Papers, 225th ACS Meeting*; New Orleans, LA, March 23−27, 2003; American Chemical Society: Washington, D.C., 2003; pp 23–27.
(15) Sellinger, A.; Tamaki, R.; Laine, R. M.; Ueno, K.; Tanabe, H.; Williams, E.; Jabbour, G. E. *Chem. Commun.* **2005**, *29*, 3700–3702.
(16) Sellinger, A.; Tamaki, R.; Laine, R. M.; Ueno, K.; Tanabe, H.; Williams, E.; Jabbour, G. E. *Materials Research Society Symposium Proceedings: Organic/Inorganic Hybrid Materials−2004*; Materials Research Society: Warrendale, PA, 2005; Vol. 847, pp 399–403.
(17) (a) Hartmann-Thompson, C.; Keeley, D.; Dvornic, P. R.; Keinath, S. E.; McCrea, K. *J. Appl. Polym. Sci.* **2007**, *104* (5), 3171–3182. (b) Hartmann-Thompson, C. U.S. Patent 0090015 A1, 2005.
(18) Shindel, C.; Zitzer, A.; Schulte, B.; Gerhards, A.; Stanley, P.; Hughes, C.; Koronakis, V.; Bhakdi, S.; Palmer, M. *Eur. J. Biochem.* **2001**, *268*, 800–808.
(19) Weber, G. *Biochem. J.* **1952**, *51* (2), 155–167.
(20) Fukumura, H.; Hayashi, K. *J. Colloid Interface Sci.* **1990**, *135* (2), 435–442. (b) Yguerabide, J.; Talavera, E.; Alvarez, J. M.; Afkir, M. *Anal. Biochem.* **1996**, *241* (2), 238–247.
(21) Ghosh, P. B.; Whitehouse, M. W. *Biochem. J.* **1968**, *108*, 155–156.
(22) Diwu, Z.; Zhang, C.; Klaubert, D. H.; Haugland, R. P. *J. Photochem. Photobiol., A* **2000**, *131* (1–3), 95–100.

thiol groups under mild conditions[24] and their wavelength of fluorescence is highly sensitive to the polarity of their immediate chemical environment. It is worth noting that several of the main scales of solvent polarity[25] are based on UV–visible wavelength shifts for a dye across a range of solvents, e.g., the SPP (solvent polarity−polarizability scale) is based on the 2-N,N-dimethyl-7-nitrofluorene/2-fluoro-7-nitrofluorene pair.[26] The fluorescent labels of Figure 1 are widely used in multiphoton excitation microscopy,[27] fluorescence labeling of biochemical and medical systems, and in a few sensing applications (e.g., molecularly imprinted sol–gels have been functionalized with NBD to create a sensor system for fluorene).[28] Using POSS to carry the fluorophores is advantageous for three reasons. First, POSS is known to be capable of forming aerosols,[29] making it suitable for threat cloud applications. Second, POSS is a nanoform of silica, and attachment of fluorophores to a nanoscaffold such as POSS will generate a system with more sensor groups per unit mass (or unit volume) and greater sensitivity than a microscaffold system. Third, when attached to a bulky POSS(isobutyl)$_7$ moiety (see Figure 1), a fluorophore is more sterically hindered than it would be if used in "free" small molecule form. Thus aggregation and resulting self-quenching of fluorescence would be expected to be reduced in a POSS−fluorophore system. This concept has also been used in biomedical fluorescence tomography, where dye molecules were loaded onto a viral nanoparticles in order to suppress fluorescence quenching.[30] However, a chemical spacer unit between the fluorophore and the nanoparticle is desirable in such cases. When a carbocyanine dye was bound to the surface of a TiO_2 nanoparticle, decreases in fluorescence yield relative to the free dye were observed and accounted for in terms of electron transfer from the excited singlet state to the nanoparticle.[31]

The fluorophores of Figure 1 readily undergo two-photon processes, i.e., absorb two photons essentially simultaneously (equivalent to the absorption of a single photon with an energy equal to the sum of the two that are absorbed).[27,32] The probability of simultaneous two-photon absorption is very low, but two-photon events can occur with high probability at the point of focus of a femtosecond pulsed laser with pulse duration shorter than 100 fs (1×10^{-13} s). At the focus, the photon density is high enough for the fluorophore to absorb two photons simultaneously, but the moderate mean power levels are low enough not to damage the sample or induce excessive photobleaching. Because two-photon excitation of the fluorophore only happens at the focus, it is possible to control the distance at which remote sensing is carried out and study different optical sections of a sample, making this an ideal technique to apply to clouds or surfaces. As well as the benefits of reduced photobleaching and optical sectioning, the technique has the additional advantages of reduced scattering and high sensitivity. Given that the probability of scattering caused by air molecules and particulates such as dust, soot, pollen, and salt from the oceans has an inverse-cubed dependence on the wavelength, the use of UV-induced one-photon fluorescence is problematic, and a near-infrared femtosecond laser source is vastly preferable. As an added benefit, scattered laser light is not coherent and therefore it is incapable of inducing two-photon excitation because this nonlinear optical process requires coherent pulsed excitation. Therefore, two-photon excited laser-induced fluorescence (LIF) provides enhanced background free imaging even in the presence of scattering particles such as dust, sand and water droplets. This method has been used for imaging through biological tissue[27b] and more recently for functional imaging.[33] Compared to absorption, LIF provides orders of magnitude greater sensitivity, and LIF has been used for the detection of fluorescence signals from single molecules[34] and for the remote identification of minerals.[35]

Experimental Section

Materials. Fluorophores were purchased from Invitrogen Molecular Probes, Inc. (Eugene, OR) and other solvents and reagents were purchased from Sigma-Aldrich, Inc. (Milwaukee, WI) and used without further purification. POSS reagents were obtained from Hybrid Plastics, Inc. (Hattiesburg, MS). Flash column chromatography was carried out using a column packed with silica gel (Davisil, grade 633, 200–425 mesh, 60Å, 99+%) and various fractions were monitored by thin layer chromatography (TLC) using ME Science aluminum-backed silica gel 60 F-254 TLC plates. Ninhydrin stain solution was prepared from 0.3 wt % ninhydrin and 3 wt % acetic acid in 2-propanol.

Characterization. ^{1}H and ^{13}C NMR spectra were recorded on a Varian Unity 400 MHz NMR spectrometer equipped with a 5 mm multinuclei probe. Solvent signals were used as internal standards and chemical shifts are reported relative to tetramethylsilane (TMS). IR spectra were recorded on a Nicolet 20DXB FTIR spectrometer and samples were prepared for analysis by solution casting onto potassium bromide discs. Electrospray mass spectra were obtained using an Agilent 1100 Series LC-MSD Ion Trap with electrospray ionization. MALDI-TOF mass spectra were measured by M-Scan, Inc. (West Chester, PA) using an Applied Biosystems Voyager DE-Pro instrument. A 2,5-dihydroxybenzoic (DHB) acid matrix was used and samples were dissolved in chloroform. UV spectra were recorded on a Varian Cary 1E UV/

(23) (a) Buck, E.; Li, J.; Chen, Y.; Weng, G.; Scarlata, S.; Iyengar, R. *Science* **1999**, *283*, 1332–1335. (b) Anderson, M. T.; Baumgarth, N.; Haugland, R. P.; Gerstein, R. M.; Tjioe, T.; Herzenberg, L. A. *Cytometry* **1998**, *33*, 435–444.
(24) Haugland, R. P. *The Handbook. A Guide To Fluorescent Probes and Labelling Technologies*, 10th ed.; Invitrogen Corp.: Eugene, OR, 2005.
(25) (a) Reichardt, C. *Solvents and Solvent Effects in Organic Chemistry*; VCH Publishers: Weinheim, Germany, 1988. (b) Drago, R. S. *J. Chem. Soc., Perkin Trans. 2* **1992**, 1827.
(26) Catalan, J.; Lopez, P.; Perez, P.; Martin-Villamil, R. *Liebigs Ann.* **1995**, 241–252.
(27) (a) Masters, B. R.; So, P. T. C. *Microsc. Res. Tech.* **2004**, *63*, 3–11. (b) Denk, W.; Strickler, J. H.; Webb, W. W. *Science* **1990**, *248*, 73–76. (c) Xu, C.; Webb, W. W. *J. Opt. Soc. Am. B* **1996**, *13* (3), 481–491.
(28) Carlson, C. A.; Lloyd, J. A.; Dean, S. L.; Walker, N. R.; Edmiston, P. L. *Anal. Chem.* **2006**, *78* (11), 3537–3542.
(29) Yang, K.; MacDonald, J. G.; Malik, S.; Huang, Y. U.S. Patent 0120915 A1,2004.
(30) Wu, C.; Barnhill, H.; Liang, X.; Wang, Q.; Jiang, H. *Opt. Commun.* **2005**, *255* (4–6), 366–374.
(31) Sudeep, P. K.; Takechi, K.; Kamat, P. V. *J. Phys. Chem. C* **2007**, *111* (1), 488–494.
(32) Prasad, P. N.; Williams, D. J., *Introduction to Nonlinear Optical Effects in Molecules and Polymers*; John Wiley and Sons, Inc.: New York, 1991; p 178.
(33) Dela Cruz, J. M.; Pastirk, I.; Comstock, M.; Lozovoy, V. V.; Dantus, M. *Proc. Natl. Acad. Sci. U.S.A.* **2004**, *101* (49), 16996–17001.
(34) Betzig, E.; Trautman, J. K. *Science* **1992**, *257*, 189–195.
(35) Seigal, H. O. Can. Patent Appl. 2355993, 2003.

vis spectrophotometer. One-dimensional fluorescence spectroscopy was carried out using an Ocean Optics LS-450 gated spectrofluorometer. Two-dimensional fluorescence spectroscopy was carried out using a Varian Cary Eclipse fluorescence spectrometer (scan rate 1200 nm/min, averaging time 0.1 s, 5 nm data interval, slit width 5 nm, 600V PMT voltage).

Laser Studies. Laser experiments were carried out using a regeneratively amplified titanium-sapphire laser (Spitfire Spectra Physics) seeded with a 45 nm fwhm 100 MHz oscillator (KM Laboratories). A multiphoton intrapulse interference phase scan (MIIPS) enabled pulse shaper[36] located between the oscillator and the amplifier was used to correct phase distortions resulting in transform limited (TL) pulses centered at 800 nm (35 fs, 750 μJ/pulse at 1 kHz) at the sample. The laser beam was attenuated and focused with a 200 mm lens to a quartz cell (1 cm path length) and the fluorescence signal was collected perpendicular to beam propagation with a miniature fiber optic spectrometer (USB 2000, Ocean Optics). Optical sections ("slices") of airbrush-generated clouds within a 5 L beaker were obtained by scanning a focused laser beam with a laser scanner (Nutfield Technologies). A scientific digital camera (Apogee Alta) with a BG40 filter (Schott) to reject scattered 800 nm beam was used to photograph the optical sections. A Badger 150 airbrush connected to a cylinder of ultrahigh purity nitrogen with the outlet pressure set to 20 psi was used to generate test clouds. When interrogating clouds, a laser setting of 200 mW was used and a quartz lens of 100 mm focal length was used to focus the beam.

Synthesis of POSS Nanosensors. *1-[6-(Dimethylamino)-2-naphthalenyl]-[3-[3,5,7,9,11,13,15-heptakis(2-methylpropyl)-pentacyclo-[9.5.1.1^{3,9}1^{5,15}1^{7,13}]octasiloxan-1-yl]propyl]thio]-1-propanone (Acrylodan POSS* **1***).* Acrylodan (0.050 g; 0.221 mmol) and thiol POSS (0.197 g; 0.221 mmol) were stirred in chloroform under nitrogen at room temperature for 8 days and at reflux for a further 6 days. Reaction progress was monitored by thin layer chromatography. Chloroform was removed in vacuo and the crude product was purified by flash column chromatography (100% chloroform) to give the desired product as a yellow solid (0.18 g; 73% yield). R_f = 0.40 ($CHCl_3$). UV ($CHCl_3$): λ_{max} (nm) 366. Fluorometer (380 nm lamp, $CHCl_3$): λ_{em} (nm) 446. IR (thin film): ν (cm^{-1}) 2956, 2929, 2905, 2868 (CH_3 and CH_2, sym and asym), 1730 (C═O), 1667, 1616, 1501, 1464, 1379 (NMe_2), 1360, 1327, 1227 (SCH_2 wag), 1105 (SiOSi asym). ^{1}H NMR ($CDCl_3$): δ 0.56–0.59 (m; Si*CH*$_2$), 0.69–0.77 (t; Si*CH*$_2$), 0.93–0.94 (d; *CH*$_3$), 1.34–1.43 (m; SiCH$_2$*CH*$_2$), 1.78–1.88 (m; C*H*), 2.57–2.61 (t; S*CH*$_2$), 2.90–2.94 (t; S*CH*$_2$), 3.09 (s; N(*CH*$_3$)$_2$), 3.30–3.34 (t; *CH*$_2$C═O), 6.86 (d; Ar*H ortho* to N(CH$_3$)$_2$), 7.14–7.17 (dd; Ar*H ortho* to N(CH$_3$)$_2$), 7.61–7.63 (d; Ar*H meta* to N(CH$_3$)$_2$), 7.77–7.79 (d; Ar*H meta* to C═O), 7.88–7.91 (dd; Ar*H ortho* to C═O), 8.30 (d; Ar*H ortho* to C═O). ^{13}C NMR ($CDCl_3$): δ 11.0 (Si*C*H$_2$), 14.1 (*C*H$_2$), 22.5 (*i*-Bu*C*), 23.0 (S*C*H$_2$), 23.8 (*i*-Bu*C*), 25.7 (*i*-Bu*C*), 28.9 (S*C*H$_2$), 30.4 (*C*C═O), 38.8 (N(*C*H$_3$)$_2$), 116.3 (Ar*C*H), 124.5 (Ar*C*H), 126.3 (Ar*C*H), 128.8 (Ar*C*H), 130.9 (Ar*C*H), 132.5 (Ar*C*H). MS (EI positive mode): *m/z* 1139 (Calcd 1140, molecular ion plus sodium).

5-(Dimethylamino)-N-[3-[3,5,7,9,11,13,15-heptakis(2-methylpropyl)pentacyclo[9.5.1.1^{3,9}.1^{5,15}.1^{7,13}]-octasiloxan-1-yl]propyl]-1-naphthalenesulfonamide (1,5-Dansyl POSS **2***).* 1-Dimethylnaphthalene-5-sulfonyl chloride (0.200 g; 0.741 mmol) and amino POSS (0.648 g; 0.741 mmol) were stirred in chloroform under nitrogen at room temperature for 12 days and at reflux for a further 14 days. Reaction progress was monitored by thin layer chromatography. Chloroform was removed in vacuo and the crude product was purified by flash column chromatography (100% chloroform) to give the desired product as an off-white solid (0.57 g; 69% yield). R_f = 0.55 ($CHCl_3$). UV ($CHCl_3$): λ_{max} (nm) 341. Fluorometer (380 nm lamp, $CHCl_3$): λ_{em} (nm) 497. IR (thin film): ν (cm^{-1}) 2955, 2920, 2897, 2866 (CH_3 and CH_2, sym and asym), 1612, 1586, 1576, 1464, 1423, 1407, 1395, 1382, 1363, 1353, 1317 (SO_2 asym), 1259, 1227, 1186 (SO_2 sym), 1111 (SiOSi asym). ^{1}H NMR ($CDCl_3$): δ 0.46–0.50 (d; Si*CH*$_2$), 0.55–0.59 (t; Si*CH*$_2$), 0.91–0.95 (m; *CH*$_3$), 1.51–1.53 (m; SiCH$_2$*CH*$_2$), 1.77–1.87 (m; *CH*), 2.84–2.88 (t; *CH*$_2$NHSO$_2$), 2.89 (s; N(*CH*$_3$)$_2$), 7.18–7.20 (d; Ar*H para* to N(CH$_3$)$_2$), 7.50–7.58 (2dd; Ar*H meta* to SO_2 and Ar*H ortho* to N(CH$_3$)$_2$), 8.23–8.25 (dd; Ar*H meta* to N(CH$_3$)$_2$), 8.27–8.29 (d; Ar*H para* to SO_2), 8.53–8.56 (d; Ar*H ortho* to SO_2). ^{13}C NMR ($CDCl_3$): δ 9.1 (Si*C*H$_2$), 22.4 (*i*-Bu*C*), 23.3 (*C*H$_2$) 23.8 (*i*-Bu*C*), 25.7 (*i*-Bu*C*), 45.1 (*C*H$_2$NHSO$_2$), 45.7 (N(*C*H$_3$)$_2$), 103.2 (Ar*C*), 114.0 (Ar*C*), 114.9 (Ar*C*), 115.3 (Ar*C*), 118.6 (Ar*C*), 122.9 (Ar*C*), 127.9 (Ar*C*), 129.7 (Ar*C*), 130.2 (Ar*C*), 130.5 (Ar*C*). MS (EI positive mode): *m/z* 1131 (Calcd 1131, molecular ion plus sodium).

6-(Dimethylamino)-N-[3-[3,5,7,9,11,13,15-heptakis(2-methylpropyl)pentacyclo[9.5.1.1^{3,9}.1^{5,15}.1^{7,13}]-octasiloxan-1-yl]propyl]-2-naphthalenesulfonamide (2,6-Dansyl POSS **3***).* 2-Dimethylaminonaphthalene-6-sulfonyl chloride (0.30 g; 1.11 mmol) and amino POSS (0.971 g; 1.11 mmol) were stirred in chloroform (5 mL) under nitrogen at room temperature for 14 days and then heated at 50 °C for 7 days . Reaction progress was monitored by thin layer chromatography. Chloroform was removed in vacuo and the crude product was purified by flash column chromatography (100% chloroform) to give the desired product as a pale orange solid (0.83 g; 67% yield). R_f = 0.25 ($CHCl_3$). UV ($CHCl_3$): λ_{max} (nm) 324. Fluorometer (380 nm lamp, $CHCl_3$): λ_{em} (nm) 427. IR (thin film): ν (cm^{-1}) 3249 ($NHSO_2$), 2955, 2924, 2896, 2863 (CH_3 and CH_2, sym and asym), 1624, 1510, 1465, 1384 ($ArNMe_2$), 1330 (SO_2), 1230 ($SiCH_2$), 1109 (SiOSi asym) 835 (SiOSi sym). ^{1}H NMR ($CDCl_3$): δ 0.52–0.55 (d; Si*CH*$_2$), 0.56–0.60 (t; Si*CH*$_2$), 0.92–0.95 (dd; *CH*$_3$), 1.57 (m; *CH*$_2$), 1.80–1.88 (m; *CH*), 2.92–2.97 (m; *CH*$_2$NHSO$_2$), 3.12 (s; N(*CH*$_3$)$_2$), 6.96–7.00 (m; Ar*H*), 7.23–7.25 (d; Ar*H*), 7.67–7.69 (dd; Ar*H*), 7.70–7.72 (d; Ar*H*), 7.79–7.82 (d; Ar*H*), 8.25 (d; Ar*H*).^{13}C NMR ($CDCl_3$): δ 9.21 (Si*C*H$_2$), 22.5, 23.8, 25.7 (Bu*C*), 23.3 (*C*H$_2$), 41.5 (*C*H$_2$NHSO$_2$), 45.6 (N(*C*H$_3$)$_2$), 117.3 (Ar*C*H), 123.1 (Ar*C*H), 127.4 (Ar*C*H), 127.6 (Ar*C*H), 128.4 (Ar*C*H), 130.6 (Ar*C*H). MS (MALDI-TOF): *m/z* 1107 (Calcd 1108).

5-(Dimethylamino)-N-[3-[3,5,7,9,11,13,15-heptakis(2-methylpropyl)pentacyclo[9.5.1.1^{3,9}.1^{5,15}.1^{7,13}]-octasiloxan-1-yl]propyl]-2-naphthalenesulfonamide (2,5-Dansyl POSS **4***).* 2-Dimethylaminonaphthalene-5-sulfonyl chloride (0.30 g; 1.11 mmol) and amino POSS (0.971 g; 1.11 mmol) were stirred in chloroform (5 mL) under nitrogen at room temperature for 7 days and then heated at 50 °C for 9 days. Reaction progress was monitored by thin layer chromatography. Chloroform was removed in vacuo and the crude product was purified by flash column chromatography (2:1 v/v chloroform-hexane) to give the desired product as a pale yellow solid (1.09 g; 89% yield). R_f = 0.10 ($CHCl_3$). UV ($CHCl_3$): λ_{max} (nm) 407. Fluorometer (380 nm lamp, $CHCl_3$): λ_{em} (nm) 452. IR (thin film): ν (cm^{-1}) 3290 ($NHSO_2$), 2954, 2926, 2900, 2866 (CH_3 and CH_2, sym and asym), 1621, 1593, 1514, 1465, 1367 ($ArNMe_2$) 1327 (SO_2), 1230 ($SiCH_2$), 1202, 1109 (SiOSi asym), 830 (SiOSi sym). ^{1}H NMR ($CDCl_3$): δ 0.47–0.51 (t; Si*CH*$_2$), 0.56–0.60 (t; Si*CH*$_2$), 0.91–0.96 (m; *CH*$_3$), 1.50–1.56 (m; *CH*$_2$), 1.78–1.88 (m; *CH*), 2.84–2.89 (m; *CH*$_2$N), 3.09 (s; N(*CH*$_3$)$_2$), 7.03 (m; Ar*H*), 7.28–7.31 (dd; Ar*H*), 7.37–7.41 (dd; Ar*H*), 7.84–7.86 (d; Ar*H*), 7.92–7.94 (d; Ar*H*), 8.50–8.52 (d; Ar*H*). ^{13}C NMR ($CDCl_3$): δ 9.2 (Si*C*H$_2$), 22.4, 23.8, 25.7 (Bu*C*), 23.3 (*C*H$_2$), 40.8 (N*C*H$_3$), 45.7 (SO$_2$N*C*H$_2$), 117.9 (Ar*C*H), 124.5 (Ar*C*H), 125.2 (Ar*C*H), 132.5

(36) (a) Pastirk, I.; Resan, B.; Fry, A.; MacKay, J.; Dantus, M. *Opt. Express* **2006**, *14*, 9537. (b) Xu, B. W.; Gunn, J. M.; Dela Cruz, J. M.; Lozovoy, V. V.; Dantus, M. *J. Opt. Soc. Am. B* **2006**, *23*, 750.

(Ar*C*H), 134.3 (Ar*C*H), 136.2 (Ar*C*H). MS (MALDI-TOF): *m/z* 1107 (Calcd 1108).

N-[3-[3,5,7,9,11,13,15-Heptakis(2-methylpropyl)pentacyclo-[9.5.1.1^{3,9}.1^{5,15}.1^{7,13}]octasiloxan-1-yl]-propyl]-1-pyrenesulfonamide (1-Pyrene POSS **5***).* 1-Pyrene sulfonyl chloride (0.400 g; 1.32 mmol) and amino POSS (1.160 g; 1.32 mmol) were stirred in chloroform under nitrogen at room temperature for 14 days. Reaction progress was monitored by thin layer chromatography. Chloroform was removed in vacuo and the crude product was purified by flash column chromatography (100% chloroform gradient to 1:1 v/v chloroform-hexane) to give the desired product as a pale yellow solid (0.80 g; 53% yield). Rf = 0.45 ($CHCl_3$). UV ($CHCl_3$): λ_{max} (nm) 356. Fluorometer (380 nm lamp, $CHCl_3$): λ_{em} (nm) 385 and 399. IR (thin film): ν (cm^{-1}) 3288 (NH), 2954, 2915, 2868, 2847 (CH_3 and CH_2, sym and asym), 1456, 1327 (SO_2 asym), 1226, 1193, 1148 (SO_2 sym), 1100 (SiOSi asym), 1033, 845, 744. ^{1}H NMR ($CDCl_3$): δ 0.41–0.47 (t; Si*C*H_2), 0.54–0.56 (t; Si*C*H_2), 0.84–0.94 (m; *C*H_3), 1.52–1.54 (m; SiCH$_2$*C*H_2), 1.70–1.85 (m; *C*H), 2.88–2.90 (t; *C*H_2NHSO$_2$), 8.08–8.12 (m; Ar*H*), 8.20–8.23 (2d; Ar*H*), 8.29–8.33 (m; Ar*H*), 8.67–8.69 (d; Ar*H*), 8.95–8.97 (d; Ar*H*). ^{13}C NMR ($CDCl_3$): δ (ppm) 9.1 (Si*C*H$_2$), 22.4 (*i*-Bu*C*), 23.3 (*C*H$_2$), 23.8 (*i*-Bu*C*), 25.7 (*i*-Bu*C*), 45.6 (*C*H$_2$NHSO$_2$), 123.0 (Ar*C*), 123.8 (Ar*C*), 124.1 (Ar*C*), 125.3 (Ar*C*), 126.8 (Ar*C*), 126.9 (Ar*C*), 127.0 (Ar*C*), 127.1 (Ar*C*), 127.5 (Ar*C*), 128.0 (Ar*C*), 130.1 (Ar*C*), 130.2 (Ar*C*), 131.0 (Ar*C*), 131.2 (Ar*C*), 134.9 (Ar*C*). MS (EI negative mode): *m/z* 1137 (Calcd 1139, molecular ion).

N-[3-[3,5,7,9,11,13,15-Heptakis(2-methylpropyl)pentacyclo-[9.5.1.1^{3,9}.1^{5,15}.1^{7,13}]octasiloxan-1-yl]-propyl]-2-anthracenesulfonamide (2-Anthracene POSS **6***).* 2-Anthracenesulfonyl chloride (1 mg; 3.61 μmol) and amino POSS (3.6 mg; 3.61 μmol) were stirred in chloroform (4 mL) under nitrogen at room temperature for 8 days and then heated at 50 °C for 3 days. Reaction progress was monitored by thin layer chromatography. Chloroform was removed in vacuo and the crude product in chloroform was purified by flash column chromatography (5:1 v/v hexane-chloroform gradient to 100% chloroform) to give the desired product as a pale yellow solid in negligible yield. MS (MALDI-TOF, 1:1 v/v MeOH-CH_2Cl_2, DHB matrix): *m/z* 1108 (Calcd 1115).

N-[3-[3,5,7,9,11,13,15-Heptakis(2-methylpropyl)pentacyclo-[9.5.1.1^{3,9}.1^{5,15}.1^{7,13}]octasiloxan-1-yl]-propyl]-7-nitro-2,1,3-benzoxadiazol-4-amine (NBD POSS **7***).* 4-Chloro-7-nitrobenzfurazan (NBD chloride, 0.401 g; 2.00 mmol) and amino POSS (1.758 g; 2.00 mmol) were stirred in chloroform under nitrogen at room temperature for 14 days. Reaction progress was monitored by thin layer chromatography. Chloroform was removed in vacuo and the crude product was purified by flash column chromatography (100% chloroform gradient to 1:1 v/v chloroform-hexane) to give the desired product as an orange solid (1.10 g; 53% yield). R_f = 0.35 ($CHCl_3$). UV ($CHCl_3$): λ_{max} (nm) 446. Fluorometer (470 nm lamp, $CHCl_3$): λ_{em} (nm) 523. IR (thin film): ν (cm^{-1}) 3250 (NH), 2955, 2912, 2870, 2849 (CH_3 and CH_2, sym and asym), 1574 (NO_2 asym), 1380, 1305 (NO_2 sym), 1288, 1254, 1094 (SiOSi asym). ^{1}H NMR ($CDCl_3$): δ 0.60–0.62 (d; Si*C*H_2), 0.74–0.78 (t; Si*C*H_2), 0.94–0.96 (m; *C*H_3), 1.80–1.90 (m; *C*H), 1.90–1.92 (m; SiCH$_2$*C*H_2), 3.50–3.51 (t; *C*H_2NHAr), 6.16–6.18 (d; Ar*H meta* to NO_2), 8.48–8.50 (d; Ar*H ortho* to NO_2). ^{13}C NMR ($CDCl_3$): δ 9.3 (Si*C*H$_2$), 22.1 (*C*H$_2$), 22.4 (*i*-Bu*C*), 23.8 (*i*-Bu*C*), 25.7 (*i*-Bu*C*), 48.9 (NH*C*H$_2$), 134.7 (Ar*C*), 136.3 (Ar*C*), 140.7 (Ar*C*), 143.2 (Ar*C*), 143.9 (Ar*C*), 144.3 (Ar*C*). MS (EI positive mode): *m/z* 1039 (Calcd 1038, molecular ion plus sodium).

4-[5-[4-(Dimethylamino)phenyl]-2-oxazolyl]-N-[3-[3,5,7,9,11,13,15-heptakis(2-methylpropyl)pentacyclo[9.5.1.1^{3,9}.1^{5,15}I^{7,13}]octasiloxan-1-yl]propyl]benzenesulfonamide (Dapoxyl POSS **8***).* Dapoxyl chloride (0.040 g; 0.110 mmol) and amino POSS (0.096 g; 0.110 mmol) were stirred in chloroform under nitrogen at room temperature for 14 days. Reaction progress was monitored by thin layer chromatography. Chloroform was removed in vacuo and the crude product was purified by flash column chromatography (1:1 v/v chloroform-hexane gradient to 100% chloroform) to give the desired product as a deep yellow solid (0.12 g; 91% yield). R_f = 0.10 ($CHCl_3$). UV ($CHCl_3$): λ_{max} (nm) 323. Fluorometer (380 nm lamp, $CHCl_3$): λ_{em} (nm) 500. IR (thin film): ν (cm^{-1}) 3300 (NH), 2964, 2913, 2885, 2846 (CH_3 and CH_2, sym and asym), 1506, 1461, 1330 (SO_2 asym), 1259, 1225, 1150 (SO_2 sym), 1099 (SiOSi asym), 1015, 801, 740. ^{1}H NMR ($CDCl_3$): δ 0.58–0.62 (m; Si*C*H_2), 0.93–0.97 (m; *C*H_3), 1.60 (m; *C*H_2), 1.81–1.86 (m; *C*H), 2.84 (t; *C*H_2NH), 3.03 (s; N(*C*H_3)$_2$); 6.74–6.78 (d; Ar*H*), 7.30 (s; Ar*H*), 7.59–7.61 (d; Ar*H*), 7.93–7.95 (d; Ar*H*), 8.19–8.21 (d; Ar*H*). ^{13C} NMR ($CDCl_3$): δ 9.6 (Si*C*H$_2$), 22.7 (*i*-Bu*C*) 23.2 (*C*H$_2$), 24.1 (*i*-Bu*C*), 25.9 (*i*-Bu*C*), 40.5 (N(*C*H$_3$)$_2$), 45.8 (*C*H$_2$NHSO$_2$), 112.3 (Ar*C*H), 115.7 (Ar*C*), 121.4 (Ar*C*H), 125.9 (Ar*C*H), 126.5 (Ar*C*H), 127.7 (Ar*C*H), 131.6 (Ar*C*), 140.9 (Ar*C*), 150.9 (oxazole Ar*C*), 153.5 (oxazole Ar*C*), 158.3 (oxazole Ar*C*). MALDI-TOF MS: *m/z* 1202 (Calc. 1201). MS (EI positive mode): *m/z* 1081 (Calcd 1081, M^+ minus PhN(CH$_3$)$_2$ fragment).

1-[[3-[[[3-[3,5,7,9,11,13,15-Heptakis(2-methylpropyl)pentacyclo[9.5.1.1^{3,9}.1^{5,15}.1^{7,13}]octasiloxan-1-yl]propyl]amino]carbonyl]phenyl]methyl]-4-[5-(4-methoxy-3-sulfophenyl)-2-oxazolyl]pyridinium, inner salt (Cascade Yellow POSS **9***).* Cascade Yellow succinimide ester (30 mg; 0.053 mmol) and amino POSS (0.0456 g; 0.053 mmol) were stirred in chloroform (5 mL) under nitrogen at room temperature for 6 days. Reaction progress was monitored by thin layer chromatography. Chloroform was removed in vacuo and the crude product was purified by flash column chromatography (100% chloroform gradient to 3:1 v/v chloroform-methanol) to give the desired product as a bright yellow powder solid (30 mg; 42% yield). R_f = 0.25 ($CHCl_3$). UV ($CHCl_3$): λ_{max} (nm) 438. Fluorometer (380 nm lamp, $CHCl_3$): λ_{em} (nm) 529. MS (EI positive mode): *m/z* 1316 (Calcd 1323, molecular ion).

Scheme 1. Preparation of Acrylodan POSS(^{i}Bu)$_7$ 1

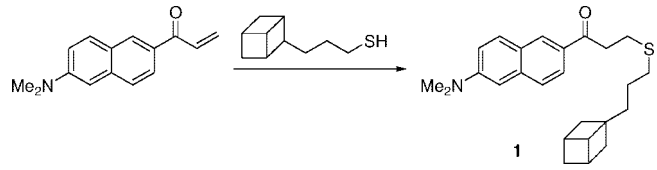

Results and Discussion

Preparation and Characterization of Nanosensor Materials. Nine POSS nanosensor materials were prepared by reacting commercially available fluorophores with amino-functionalized or thiol-functionalized POSS reagents. The materials were characterized by IR, ^{1}H and ^{13}C NMR, mass spectrometry, and UV and fluorescence spectroscopy. Acrylodan POSS **1** was prepared by reacting acrylodan with thiol POSS in chloroform (Scheme 1). The disappearance of the acrylate carbonyl (1640−1700 cm^{-1} region) and the appearance of the ketone carbonyl at 1730 cm^{-1} was observed in the IR spectrum, and the expected molecular ion was observed by electrospray mass spectrometry. The ^{1}H and ^{13}C NMR spectra were also consistent with the formation of two methylene groups alpha to a thioether and an aryl ketone (2.9 and 3.3 ppm in the proton spectrum, and 29 and 30 ppm in the carbon spectrum). 1,5-Dansyl POSS **2**, 2,6-dansyl POSS **3** and 2,5-dansyl POSS **4** were prepared by reacting

Scheme 2. Preparation of 1,5-Dansyl POSS(^{i}Bu)$_7$ 2

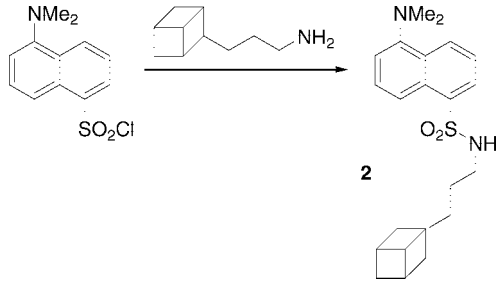

Scheme 3. Preparation of Pyrene POSS(^{i}Bu)$_7$ 5

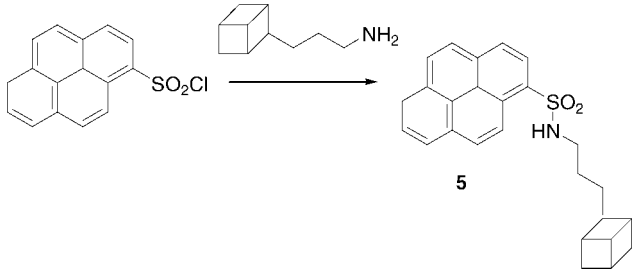

Scheme 4. Preparation of NBD POSS(^{i}Bu)$_7$ 7

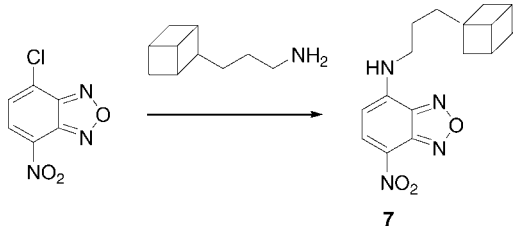

the appropriate dimethylaminonaphthalene sulfonyl chloride with amino POSS in chloroform to form the sulfonamide (e.g., 1,5-dansyl POSS **2**, Scheme 2), and the expected molecular ion was observed by mass spectrometry in all three cases. The ^{1}H and ^{13}C NMR spectra indicated the presence of a methylene group alpha to a sulfonamide (2.8 to 2.9 ppm in the proton spectrum, and 40−5 ppm in the carbon spectrum). 1-Pyrene POSS **5** and 2-anthracene POSS **6** were prepared by reacting the appropriate sulfonyl chloride with amino POSS in chloroform to form the sulfonamide (e.g., 1-pyrene POSS **5**, Scheme 3), and the molecular ion was observed by electrospray mass spectrometry in both cases. NBD POSS **7** was prepared by reacting NBD chloride with amino POSS in chloroform (Scheme 4), and the molecular ion plus sodium was observed by electrospray mass spectrometry. The ^{1}H and ^{13}C NMR spectra indicated the presence of a methylene alpha to ArNH (3.5 ppm in the proton spectrum, and 49 ppm in the carbon spectrum). Dapoxyl POSS **8** was prepared by reacting dapoxyl chloride with amino POSS (Scheme 5). ^{1}H and ^{13}C NMR suggested that the desired product had formed (presence of methylene carbon and protons alpha to sulfonamide, and the expected ratio of aromatic to aliphatic integrals), and the molecular ion was observed by MALDI-TOF mass spectrometry. In this case, the molecular ion was not observed by electrospray mass spectrometry. However, a fragment of mass 1081 was observed in the positive mode, consistent with the loss of dimethylphenylamine ($PhNMe_2$) from the desired product.

Scheme 5. Preparation of Dapoxyl POSS(^{i}Bu)$_7$ 8

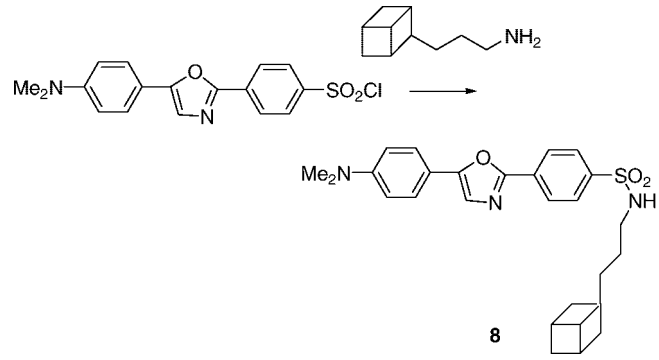

Scheme 6. Preparation of Cascade Yellow POSS(^{i}Bu)$_7$ 9.

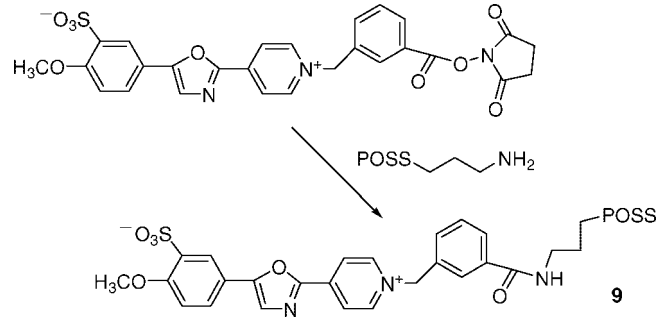

Cascade Yellow POSS **9** was prepared by reacting the succinnimidyl ester derivative with amino POSS in chloroform (Scheme 6), and the expected molecular ion was observed by electrospray mass spectrometry. Because of the microscale of the anthracene and Cascade Yellow reactions, these products were not characterized by NMR or IR spectroscopy.

Because of the sensitivity of fluorescence techniques, it was essential that all of the nanosensors were of high purity. Compounds **1**−**8** were purified by flash column chromatography with chloroform or chloroform−hexane as the elution solvent, and a chloroform−methanol system was used for compound **9**. A ninhydrin thin layer chromatography stain test was used to show that compounds **2**−**9** were free of unreacted amino POSS. Amino POSS gives a burgundy spot at $R_f = 0$ when eluted in chloroform, dipped in ninhydrin and heated to 100 °C. No such spot was observed in compounds **2**−**9**.

When characterizing novel fluorophores, it is common to quote fluorescence lifetime and quantum yield. However, the fluorescence lifetimes and quantum yields of numerous amine derivatives of dansyl,[37–40] dapoxyl,[41] and pyrene[42] (and the thiol derivatives of acrylodan[43]) have been extensively

(37) Parker, C. W.; Yoo, T. J.; Johnson, M. C.; Godt, S. M. *Biochemistry* **1967**, *6* (11), 3408–3416.
(38) Chen, R. F. *Arch. Biochem. Biophys.* **1968**, *128* (1), 163–175.
(39) Herron, J. N.; Voss, E. W. *J. Biochem. Biophys. Methods* **1981**, *5* (1), 1–17.
(40) Homachaudhuri, L.; Kumar, S.; Swaminathan, R *FEBS Lett.* **2006**, *580* (8), 2097–2101.
(41) Diwu, Z.; Lu, Y.; Zhang, C.; Klaubert, D. H.; Haughland, R. P. *Photochem. Photobiol.* **1997**, *66* (4), 424–431.
(42) Andreoni, A.; Bottiroli, G.; Colasanti, A.; Giangare, M. C.; Riccio, P.; Roberti, G.; Vaghi, P *J. Biochem. Biophys. Methods* **1994**, *29* (2), 157–172.
(43) Prendergast, F. G.; Meyer, M.; Carlson, G. L.; Iida, S.; Potter, J. D. *J. Biol. Chem.* **1983**, *258* (12), 7541–7544.

Table 1. Fluorescence Data (absolute and relative to chloroform) for POSS Nanosensor Compounds Exposed to Various Analytes

	λ_{em} (nm)											
	acrylodan POSS **1**		1,5-dansyl POSS **2**		2,6-dansyl POSS **3**		2,5-dansyl POSS **4**		NBD POSS **7**[a]		dapoxyl POSS **8**	
$CHCl_3$	446	0	497	0	427	0	452	0	523	0	500	0
hexane	421	−25	448	−49	414	−13	429	−23	504	−19	437	−63
toluene	437	−9	496	−1	425	−2	444	−8	514	−9	492	−8
xylene	437	−9	496	−1	427	0	443	−9	519	−4	492	−8
acetone	451	+5	492	−5	439	+12	490	+38	525	+2	542	+42
MeOH	509	+63	523	+26	437	+10	493	+41	536	+13	554	+54
EtOH	502	+56	509	+12	439	+12	490	+38	533	+10	534	+34
water	490	+44	494	−3	insoluble		insoluble		542	+19	517	+17
MeCN	487	+41	514	+17	441	+14	492	+40	530	+7	555	+55
CEES	451	+5	496	−1	433	+6	483	+31	524	+1	510	+10
acephate	498	+52	533	+36					549	+26	543	+43
DFP	470	+24	495	−2	438	+11	490	+38	558	+35	498	−2
DMMP	489	+43	502	+5	441	+14	492	+40	534	+11	503	+3
1-PrOH	500	+54	508	+11	437	+10	489	+37	532	+9	531	+31
2-PrOH	496	+50	514	+17	437	+10	490	+38	532	+9	541	+41
1-BuOH	498	+52	514	+17	436	+9	489	+37	533	+10	535	+35
2-BuOH	494	+48	511	+14	437	+10	488	+36	531	+8	531	+31
Et_2O	430	−16	495	−2	425	−2	443	−9	512	−11	495	−5
HFIP	536	+90	500	+3	447	+20	504	+52	546	+23	539	+39

[a] λ_{ex} = 380 nm in all experiments except for NBD POSS **7**, where λ_{ex} = 470 nm.

discussed elsewhere and have not been included in this study. Both the fluorescence lifetime and quantum yield of these derivatives are known to be highly solvent dependent. For example, the butylamine derivative of 1,5-dansyl chloride has a quantum yield of 0.45 in dioxane, 0.28 in methanol, and 0.03 in water,[37] and the fluorescence lifetimes of the 2,6-dansyl derivatives vary greatly with pH.[40]

One-Photon Fluorescence Fingerprints. In this study, an array is defined as a set of *n* POSS nanosensors, and a fingerprint for a given analyte is defined as the set of *n* emission wavelength (λ_{em}) data points that the set of *n* POSS nanosensors gives in response to that analyte. Fingerprints were constructed by measuring the fluorescence emission maxima (λ_{em}) of each nanosensor with each analyte of interest (Table 1). Experiments were performed by dissolving the nanosensor in the analyte at 1×10^{-4} M, placing the solution in a cuvette and measuring its fluorescence emission spectrum upon irradiation at 380 or 470 nm (see values on the left of each column in Table 1). Chloroform was selected as an arbitrary reference analyte, and fingerprints were constructed using wavelength shifts relative to chloroform for ease of visual presentation (see values on the right of each column in Table 1). The set of four nanosensors, acrylodan POSS **1**, 1,5-dansyl POSS **2**, NBD POSS **7**, and dapoxyl POSS **8** was selected to form the array. Hence, for example, a fingerprint for hexane would be constructed as follows: acrylodan POSS **1**, −25 nm (difference between 446 and 421 nm in Table 1); 1,5-dansyl POSS **2**, −49 nm (difference between 497 and 448 nm); NBD POSS **7**, −19 nm (difference between 523 and 504 nm); and dapoxyl POSS **8**, −63 nm (difference between 500 and 437 nm). This data set can be depicted as shown in Figure 2 for the topmost analyte (hexane). It should be noted that if a different reference analyte were to be chosen, or if no reference analyte were to be used (i.e., if absolute fluorescence emission wavelengths appeared on the *x*-axis), the fingerprint patterns would stay the same and only the numbers on the *x*-axis would be altered.

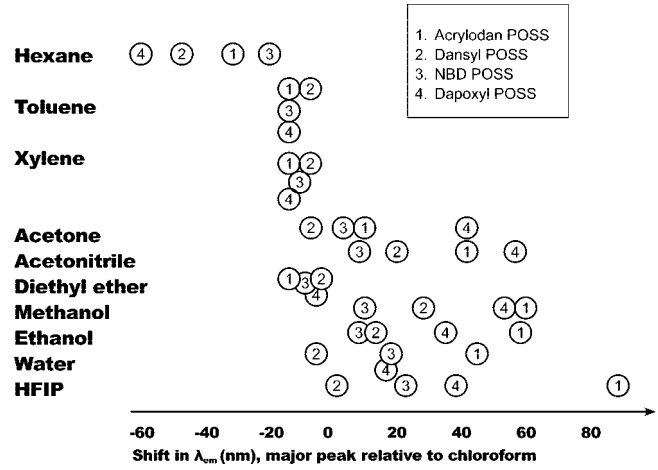

Figure 2. Fingerprints for a range of common organic compounds.

The set of four nanosensors, acrylodan POSS **1**, 1,5-dansyl POSS **2**, NBD POSS **7**, and dapoxyl POSS **8**, were selected because they could generate an array with maximum orthogonality and minimum redundancy. 1-Pyrene POSS **5** and 2-anthracene POSS **6** were not selected owing to excimer formation and the presence of multiple maxima in their emission spectra. For the set of naphthalene-based POSS nanosensors (compounds **1**−**4**), similar patterns in wavelength shifts were observed for the acrylodan POSS **1** and 2,5-dansyl POSS **4** pair, and for the 1,5-dansyl POSS **2** and 2,6-dansyl POSS **3** pair (Table 1). The degree to which a pair of fluorophores shows a similar wavelength shift pattern may be determined by counting how many wavelength shifts in a set are within *x* nm of each other. If *x* is set to an arbitrary value of 20 nm, it can be seen that acrylodan POSS **1** wavelength shifts track those of 2,5-dansyl POSS **4** for twelve out of sixteen analytes, and 1,5-dansyl POSS **2** wavelength shifts track those of 2,6-dansyl POSS **3** for 15 out of 16 analytes. Hence one component from each of the two pairs above would be redundant in the array, and 2,6-dansyl POSS **3** and 2,5-dansyl POSS **4** were excluded from the array while acrylodan POSS **1** and 1,5-dansyl POSS **2** were included because of their superior solubility in water

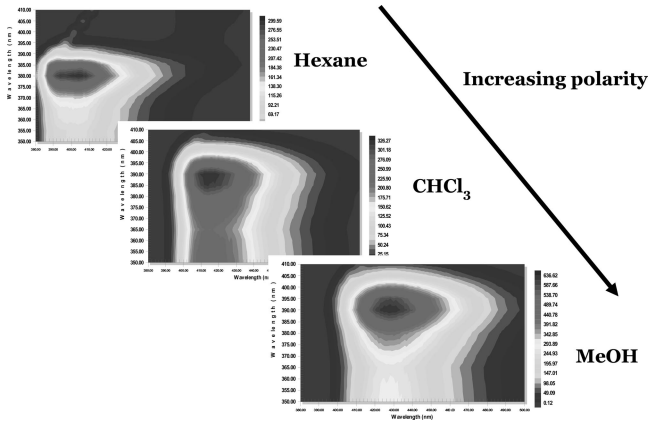

Figure 3. Two-dimensional fluorescence spectra of 2,6-dansyl POSS **3** in different solvents.

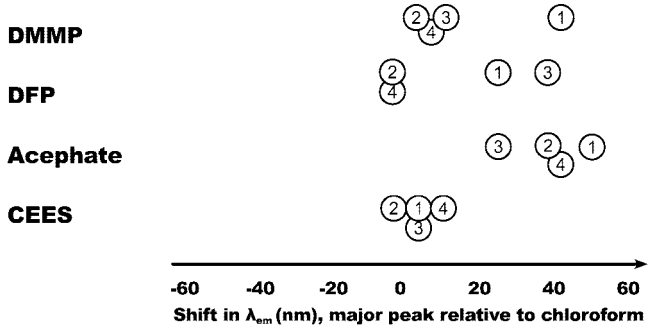

Figure 4. Fingerprints for a range of chemical warfare agent simulants.

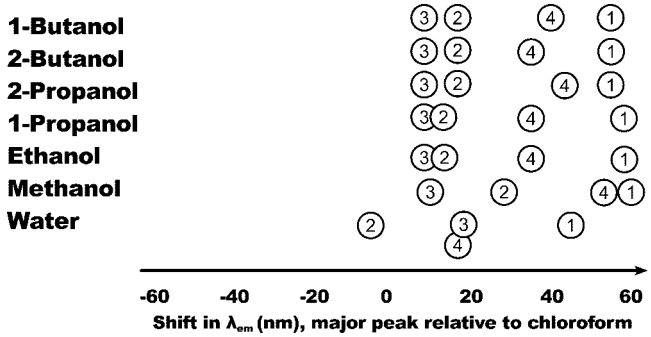

Figure 5. Fingerprints for water and a homologous series of alcohols.

(Table 1). Cascade Yellow POSS **9** was excluded from the array for reasons of limited availability.

For the purposes of this study, wavelength differences of 5 nm or less were defined as being within experimental error, and pairs of responses within 5 nm of each other were defined as being the same. It is essential that the excitation wavelength (λ_{ex}) be kept constant as the analyte is varied for a given nanosensor, since the value of λ_{em} is affected by the value of λ_{ex}. This is illustrated by the two-dimensional fluorescence spectra for 2,6-dansyl POSS **3** in Figure 3.

Array Selectivity. The selectivity of the array was studied in three sets of experiments (Table 1 and Figures 2, 4, and 5). In the first set of experiments, a number of organic solvents of varying polarities were studied, several of which fall into the category of toxic industrial chemicals (TICs), of importance in real-life detection applications (Figure 2). With the exception of toluene, xylene, and diethyl ether, (which gave near identical fingerprints clustered in the 0 to −10 nm region), the array was successfully able to distinguish these analytes. Interestingly, it was found that Cascade Yellow POSS **9** was able to distinguish toluene from diethyl ether; toluene gave a response of 519 nm (−10 nm relative to chloroform at 529 nm) and ether gave a response of 488 nm (−41 nm relative to chloroform). Hence in an application where differentiation of toluene and ether is of key importance, Cascade Yellow POSS **9** could be added to the array. The responses of the less polar analytes fell into the negative wavelength shift region, and the responses of the more polar analytes fell into the positive wavelength shift region, as expected.[25,26] This trend is also apparent in the two-dimensional fluorescence spectra shown in Figure 3.

In a second set of experiments, the array was tested with four chemical warfare agent simulants (Figure 4): dimethyl methylphosphonate and diisopropylfluorophosphate (DMMP and DFP, simulants of G series nerve agents such as soman GD, tabun GA, and sarin GB), O,S-dimethyl acetylphosphoramidothioate (acephate, a simulant of the V series nerve agent VX), and chloroethyl ethyl sulfide (CEES, a simulant of mustard gas HD).[44] The array had good selectivity for all four simulants, and it was particularly notable that the three phosphonate nerve simulants gave markedly different fingerprints, since distinguishing G agents from VX is an ongoing challenge in the field of nerve agent detection.[45,46] Other methods of nerve agent detection include surface acoustic wave sensors (SAWs),[47] and reaction between an organophosphate P−F group and indicator molecules such that the indicator molecules and indicator−organophosphate products fluorescence at different wavelengths.[48] SAWs are not G or V agent selective, because the sensing event involves the formation of a hydrogen bond between a hydrogen-bond acidic sensor coating and a hydrogen-bond basic phosphonate vapor phase molecule (G agent, V agent, or pesticide), and the indicator molecule method is not G or V agent selective because both G and V agents contain reactive P−F groups.

Since the first set of experiments (Figure 2) had demonstrated that the array could successfully distinguish water, methanol and ethanol, alcohols were studied in greater detail in the third set of experiments (Figure 5). In this case, the array could distinguish a homologous series of alcohol isomers up to 1- and 2-butanol, with the exception of the ethanol and 1-propanol pair, which gave identical fingerprints.

Nanosensor Mixtures. In real-life fluorescence detection applications, the half λ_{max} parameter is an important consideration. This is the wavelength difference between the fluorescence peak maximum and the point at which it falls to half-maximum intensity, and gives an indication of peak width. Because an array will generate a number of overlapping maxima, narrow peaks are desirable since wide overlapping peaks will be harder to distinguish. In this system, the

(44) Ghosh, T. K.; Prelas, M. A.; Viswanath, D. S.; Loyalka, S. K.; *Science and Technology of Terrorism and Counterterrorism*, Marcel Dekker, Inc.: New York, 2002; pp 324–325..
(45) Yang, Y. C. *Acc. Chem. Res.* **1999**, *32* (2), 109–115.
(46) Hopkins, A. R.; Lewis, N. S. *Anal. Chem.* **2001**, *73* (5), 884–892.
(47) McGill, R. A.; Abraham, M. H.; Grate, J. W. *CHEMTECH* **1994**, *24*, 27–37.
(48) Zhang, S.-W.; Swager, T. M *J. Am. Chem. Soc.* **2003**, *125* (12), 3420–3421.

half λ_{max} was estimated to be approximately 25 nm on the basis of the one-dimensional fluorescence spectra measured. The one-dimensional fluorescence spectra of several one to one mass mixtures of nanosensors in chloroform at $\sim 1 \times 10^{-4}$ M were measured, and separate peaks could be readily resolved when $\Delta\lambda_{em} > 30$ nm for a given pair of nanosensors. Hence, for example, acrylodan POSS **1** ($\lambda_{em} = 446$ nm) and NBD POSS **7** ($\lambda_{em} = 523$ nm) were resolved, whereas 1,5-dansyl POSS **2** ($\lambda_{em} = 497$ nm) and NBD POSS **7** ($\lambda_{em} = 523$ nm) were not.

Stability and Sensitivity. Compounds **1** to **9** were stored in the dark, and studied by thin layer chromatography at monthly intervals for the presence of decomposition (photobleaching) products. The reproducibility of the data in Table 1 was checked in two ways. First, the fluorescence spectrum of a given nanosensor−analyte pair was rerun by making up a new solution from an existing batch of nanosensor several months after the first fluorescence spectrum was taken, and comparing the two spectra. Second, when new batches of nanosensor were prepared, their fluorescence spectra with various analytes were compared with the equivalent fluorescence spectra measured using previous batches of nanosensor with the same analytes. In all cases, array reproducibility was observed within the range of experimental error (i.e., 5 nm as defined previously).

A sensitivity study was carried out on NBD POSS **7**. The concentration of a 1×10^{-4} M solution of NBD POSS **7** in chloroform was gradually reduced until no fluorescence spectrum could be detected. A 523 nm peak was visible down to a concentration of 1×10^{-9} M (1000 ppm), although it should be understood that this figure is a function of the fluorescence spectrometer arrangement as well as the nanosensor-analyte system itself. The two-dimensional fluorescence spectrum alluded to earlier in this report (Figure 3) was obtained using a 5×10^{-11} M (50 ppm) nanosensor−analyte solution.

Two-Photon Fluorescence Solution Experiments. To test the feasibility of using POSS nanosensor materials in remote detection applications, we studied the two-photon fluorescence of selected nanosensor−analyte pairs in solution, in clouds, and on surfaces using a pulsed femtosecond IR laser. Cuvettes (1 cm) of 1×10^{-4} M nanosensor−chloroform solutions were placed at a distance from the laser source, and fluorescence was monitored by a probe at a distance from the cuvette. The solutions exhibited localized fluorescence when excited by the laser beam, and showed no evidence of decomposition or decrease in fluorescence after 30 min of exposure. The remote fluorescence probe detected changes in the wavelength of fluorescence as DMMP was gradually added to the chloroform solution. Figures 6 and 7 show the change in fluorescence response as DMMP was added to chloroform solutions of NBD POSS **7** and dapoxyl POSS **8**, respectively.

Two-Photon Fluorescence Cloud Experiments. A femtosecond laser was used to interrogate clouds. An airbrush was charged with a 1×10^{-3} M solution of NBD POSS **7** in chloroform, and 1 mL solution was sprayed into a covered 5 L glass beaker, thus generating a nanosensor concentration of 2×10^{-7} mol per L in the beaker. The beaker was placed

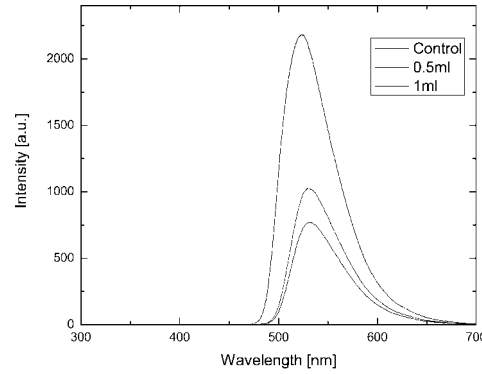

Figure 6. Remote detection experiment for NBD POSS **7** chloroform solution with addition of DMMP. Top, $CHCl_3$ control solution, no DMMP; middle, 0.5 mL of DMMP added to $CHCl_3$ solution; bottom, 1.0 mL of DMMP added to $CHCl_3$ solution.

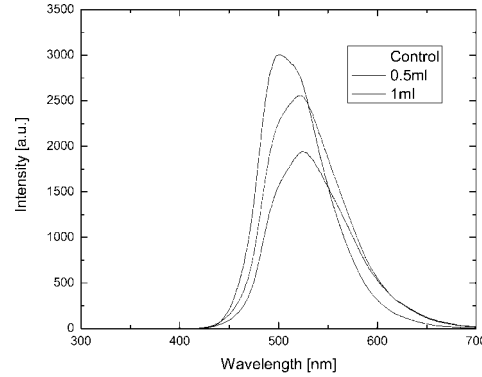

Figure 7. Remote detection experiment for dapoxyl POSS **8** chloroform solution with addition of DMMP. Top, $CHCl_3$ control solution, no DMMP; middle, 0.5 mL of DMMP added to $CHCl_3$ solution; bottom, 1.0 mL of DMMP added to $CHCl_3$ solution.

1 m from the laser source, and fluorescence was monitored by a probe 0.5 m from the beaker. When a 1×10^{-4} M solution was used in the airbrush, fluorescence was of insufficient intensity for the fluorimeter to generate a signal. A number of possible outcomes may occur when the laser interrogates a fluorophore cloud. (1) The laser beam may not be visible, indicating a lack of two-photon fluorescence (caused by insufficient fluorophore concentration or incorrect laser focusing). (2) A long white beam may be visible across the whole diameter of the beaker, indicating the chemical decomposition of the fluorophore (caused by excessive laser power). (3) A long colored beam (i.e., the color of the expected fluorescence) may be visible across the whole diameter of the beaker, indicating that delocalized two-photon fluorescence is occurring, but that laser variables (such as the focal length of the lens) are not set correctly to enable localized two-photon fluorescence. (4) The desired outcome is that the cloud in the beaker fluoresces at the desired wavelength around the point at which the laser is focused. In this experiment, a characteristic yellow-green (523 nm) laser line approximately 1 in. in length was observed in the center of the beaker, demonstrating that laser interrogation of a defined area of the cloud was feasible. To demonstrate the remote detection of a cloud of the nerve simulant DMMP by NBD POSS **7**, we repeated the procedure above using NBD POSS **7**, chloroform, and DMMP in the beaker. The wavelength of fluorescence changed in the presence of

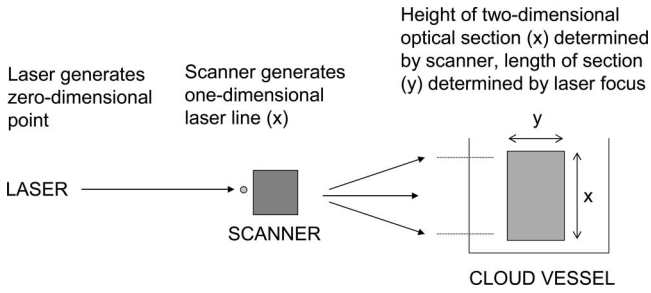

Figure 8. Generation of an optical section in a cloud vessel using a laser and laser scanner.

DMMP, and a one inch yellow (531 nm) line was observed in the center of the beaker. Thus it was shown that NBD POSS **7** was able to send a fluorescence signal to a remote fluorimeter, indicating that DMMP was present in a specific part of a cloud. The fluorescence in the center of the beaker was monitored, and persisted for 20 min, after which time the experiment was discontinued. Experiments of the type described above were repeated, except that two-dimensional fluorescent optical sections of clouds were studied instead of one-dimensional ~1 in. laser lines. Optical sections were generated using a laser scanner as outlined in Figure 8. In one experiment, a fluorescent optical section of a cloud of NBD POSS **7** responded to the presence of DMMP by giving an 8 nm yellow-green (523 nm) to yellow (531 nm) wavelength shift as above. In a second experiment, a fluorescent optical section of a cloud of dapoxyl POSS **8** responded to the presence of DMMP by giving a 25 nm blue-green (500 nm) to yellow-green (525 nm) wavelength shift.

Two-Photon Fluorescence Surface Experiments. The laser was also used to interrogate surfaces. Two black anodized aluminum samples were sprayed with either a 1×10^{-3} M solution of NBD POSS **7** in chloroform, or a 1×10^{-3} M solution of dapoxyl POSS **8** in chloroform, respectively. These control coatings were remotely interrogated by the laser, and the fluorescence was remotely monitored. The coatings were then contaminated with DMMP, reinterrogated, and changes in the fluorescence were noted (Table 2).

Table 2. Fluorescence Behavior of Nanosensor Coatings on Black Anodized Aluminum before and after DMMP Contamination

nanosensor	control coating response	coating response after DMMP contamination
NBD POSS **7**	yellow-green (523 nm)	yellow (531 nm)
dapoxyl POSS **8**	blue-green (500 nm)	yellow-green (525 nm)

Conclusions

Nine POSS nanosensor compounds that change their wavelength of fluorescence emission in response to their chemical environment were synthesized, purified and fully characterized. An array of four of these POSS nanosensors was used to generate fingerprints for a diverse range of analytes including common organic solvents, toxic industrial chemicals (TICs), chemical warfare agent simulants, and a homologous series of alcohols. The array showed excellent selectivity, and could successfully distinguish between different phosphonates and different alcohols. The array gave reproducible data, and responses for analyte concentrations of 1000 ppm and above. The feasibility of using the array for remote detection of analytes in clouds and on surfaces was demonstrated using a remote femtosecond infrared laser to induce localized two-photon fluorescence in the nanosensors and a remote probe to detect the nanosensor fluorescence responses.

Acknowledgement. . We thank Dr. Edward S. Wilks for his advice on names for the structures, which are based on the nomenclature principles published by Chemical Abstracts.

CM703641S